

NANO EXPRESS

Open Access

Fabrication and ultraviolet photoresponse characteristics of ordered SnO_x ($x \approx 0.87, 1.45, 2$) nanopore films

Changli Li¹, Maojun Zheng^{1*}, Xianghu Wang², Lujun Yao¹, Li Ma³ and Wenzhong Shen¹

Abstract

Based on the porous anodic aluminum oxide templates, ordered SnO_x nanopore films (approximately 150 nm thickness) with different x ($x \approx 0.87, 1.45, 2$) have been successfully fabricated by direct current magnetron sputtering and oxidizing annealing. Due to the high specific surface area, this ordered nanopore films exhibit a great improvement in recovery time compared to thin films for ultraviolet (UV) detection. Especially, the ordered SnO_x nanopore films with lower x reveal higher UV light sensitivity and shorter current recovery time, which was explained by the higher concentration of the oxygen vacancies in this SnO_x films. This work presents a potential candidate material for UV light detector.

PACS: 81.15.Cd, 81.40.Ef, 81.70.Jb, 85.60.Gz.

Keywords: highly ordered tin oxide nanopores films, anodized aluminum oxide(aao), ultraviolet(uv) response, oxygen vacancies

Background

Tin oxide is a wide band-gap (3.6 eV) *n*-type semiconductor and exhibits unique electrical and optical properties. It has been used extensively for gas sensors [1-4], solar cells [5], optoelectronic devices [6], catalysts [7], lithium-ion batteries [8], and so forth. In the last few years, intensive attention has been paid to fabricate a variety of SnO₂ nanostructured materials, such as nanowires [9], nanobelts [10], nanoribbons [11], nanotubes [9,12], nanoparticles [13], and nanowhiskers [14]. However, little attention had been paid to 2D ordered SnO₂ porous nanomaterials as electronic and chemical devices. 2D ordered porous nanostructures with well-aligned interconnected pores are of great potential applications due to several distinctive properties such as high internal surface areas, high gas sorption and separation capacity, and increased thermal and mechanical stabilities [15]. Herein, we firstly report the fabrication and UV photoconductivity switching properties of highly

ordered SnO_x nanopore films. Figure 1 shows the formation process of the highly ordered SnO_x nanopore films. The recovery time of this ordered SnO_x nanopore films for UV detection is much shorter than that of SnO_x thin films and we also found that the films with lower x exhibit higher UV sensitivity and faster current recovery. The results indicate that ordered SnO_x nanopore film with low x could be as potential candidate material for UV light sensors.

Methods

The AAO templates were prepared through stable high-field anodization in a H₃PO₄-H₂O-C₂H₅OH electrolyte system [16]. Anodization was carried out in a H₃PO₄-H₂O-C₂H₅OH electrolyte system (concentration of H₃PO₄, 0.25 M) at 195 V. The temperatures of the electrolytes were kept at -10°C to 0°C with a powerful low-constant temperature bath. Sn films were deposited on AAO substrates by direct current (DC) magnetron sputtering using a circular tin target (diameter, 60 mm; purity, 99.99%) at room temperature. The base pressure, deposition pressure, substrate-target distance, sputtering power, and the Ar flux were 1×10^{-3} Pa, 0.85 Pa, 6 cm, 30 W, and 10 sccm, respectively. The sputtering time (t)

* Correspondence: mjzheng@sjtu.edu.cn

¹Laboratory of Condensed Matter Spectroscopy and Opto-Electronic Physics, Department of Physics, Shanghai Jiao Tong University, Shanghai, 200240, People's Republic of China

Full list of author information is available at the end of the article

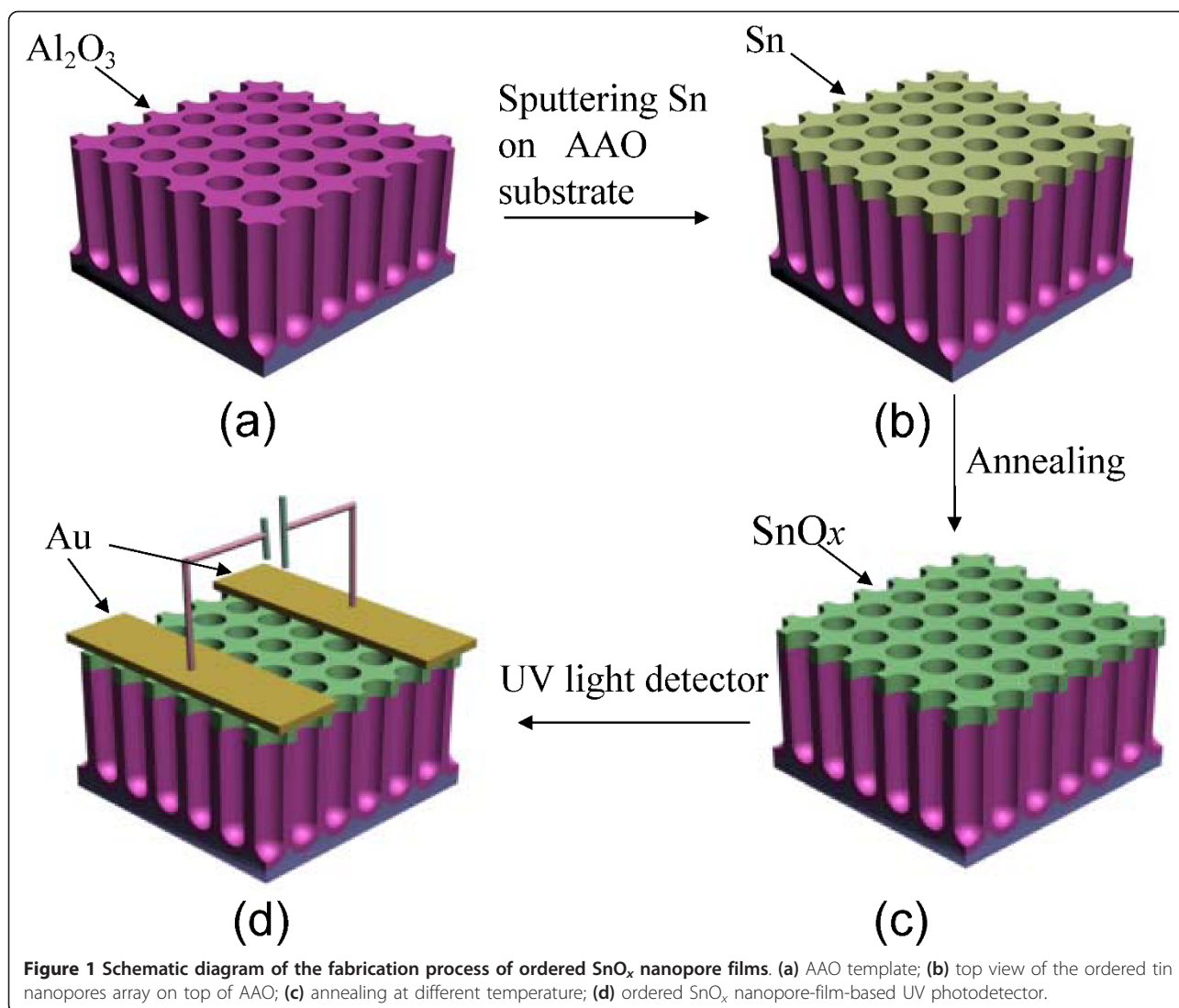


Figure 1 Schematic diagram of the fabrication process of ordered SnO_x nanopore films. (a) AAO template; (b) top view of the ordered tin nanopores array on top of AAO; (c) annealing at different temperature; (d) ordered SnO_x nanopore-film-based UV photodetector.

was fixed at 3 min. To obtain the ordered porous SnO_x films and to perform its electrical measurements under UV irradiation, three same samples was annealed at 350°C, 450°C, and 550°C in a quartz tube furnace system for 120 min at a heating rate of 10°C/min, respectively. The quartz tube was evacuated to about 50 Pa before heating and the flow rates of Ar and O₂ are both fixed at 100 sccm during annealing. Then a 300-nm-thick gold electrodes was evaporated on the surface of SnO_x nanopore films through a shadow mask and copper wires were connected to the electrodes at two contact pads by conducting silver glue. The spacing between the electrodes was 1 mm, and the length of the electrodes was 5 mm. The device structure is depicted in Figure 1d. What's more, SnO_x thin films UV device on the quartz substrate were prepared under the same deposition and post-annealing condition as mentioned above for the purposes of comparison. Electrical measurements

of all devices were carried out with a Keithley 2400 source-measure unit under ambient conditions. For UV detection, a xenon lamp was used as the light source and an excitation filter centered at 254 nm and the bias voltage was fixed at 1 V. The structural properties were determined using a D8 DISCOVER X-ray diffractometer (XRD) with Cu K α radiation. The growth and surface morphologies were observed using a field-emission scanning electron microscope (FE-SEM, Philips Sirion 200, Philips, Holland, Netherlands). The Raman spectra of the SnO_x nanostructures were measured using a Jobin Yvon LabRam HR 800 UV system with a 325 nm He-Cd laser.

Results and discussions

Surface topography

Figure 2a, b is the top view and cross-sectional FE-SEM images of a typical AAO template consisting of a

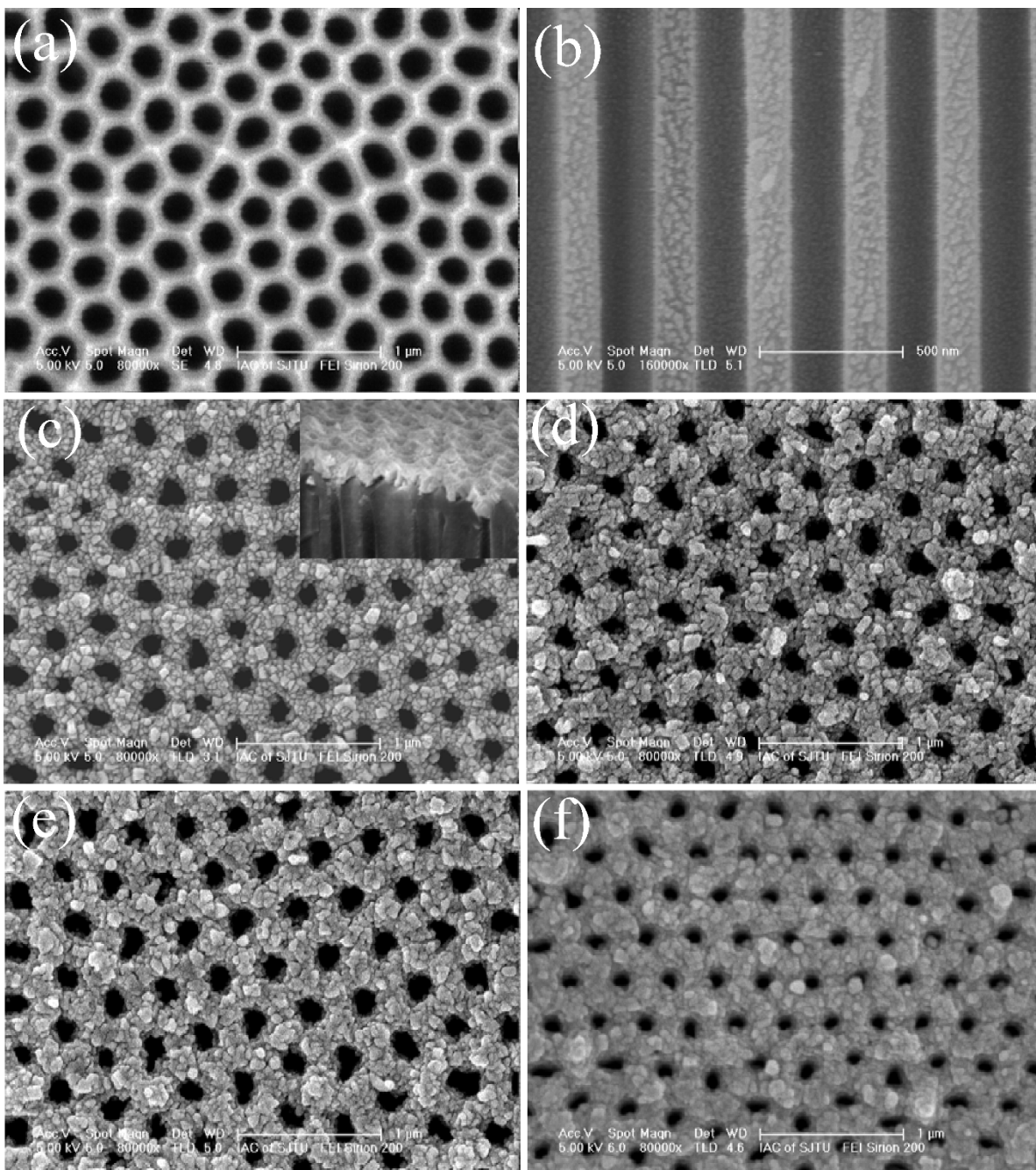


Figure 2 FE-SEM images of the AAO templates, ordered Sn and SnO_x nanopore films. **(a)** top view of the alumina template prepared by a two-step anodization method; **(b)** cross-section view of the resultant highly ordered nanochannel alumina template; **(c)** ordered Sn nanopore film prepared at room temperature with P = 30 W and t = 3 min. **(d, f)** the top images of the ordered SnO_x nanopore films prepared at different annealing temperatures (350°C, 450°C, and 550°C, respectively).

hexagonal close-packed arrays formed by the two-step anodization process. The as-grown AAO film has a large pore diameter of approximately 170 nm and interpore spacing of approximately 350 nm, the parallel cylindrical nanochannels can be clearly observed. Figure 2c shows the FE-SEM image of Sn nanopore film on an

AAO substrate. The cross-section (the inset of Figure 2c) reveals clearly that the Sn nanopores are on top of the AAO substrates. It is noted that the as-deposited Sn nanopore films consist of small grains and the obtained Sn films just reproduce the substrate geometry. While the pore diameter (approximately 150 nm) of Sn

nanopore film is smaller than the pore size of the AAO substrate. Figure 2d, e, f show the surface morphology of the annealed ordered porous Tin films at different temperatures (350°C, 450°C, and 550°C). It can be seen that the grain size of the samples annealed at 350°C was bigger than that of as-deposited Sn films and the neighboring grains seemed to coalescence together as the annealing temperature rises. The surface of the film becomes very smooth and the pore size of the film decreases when annealing temperature was increased to 550°C.

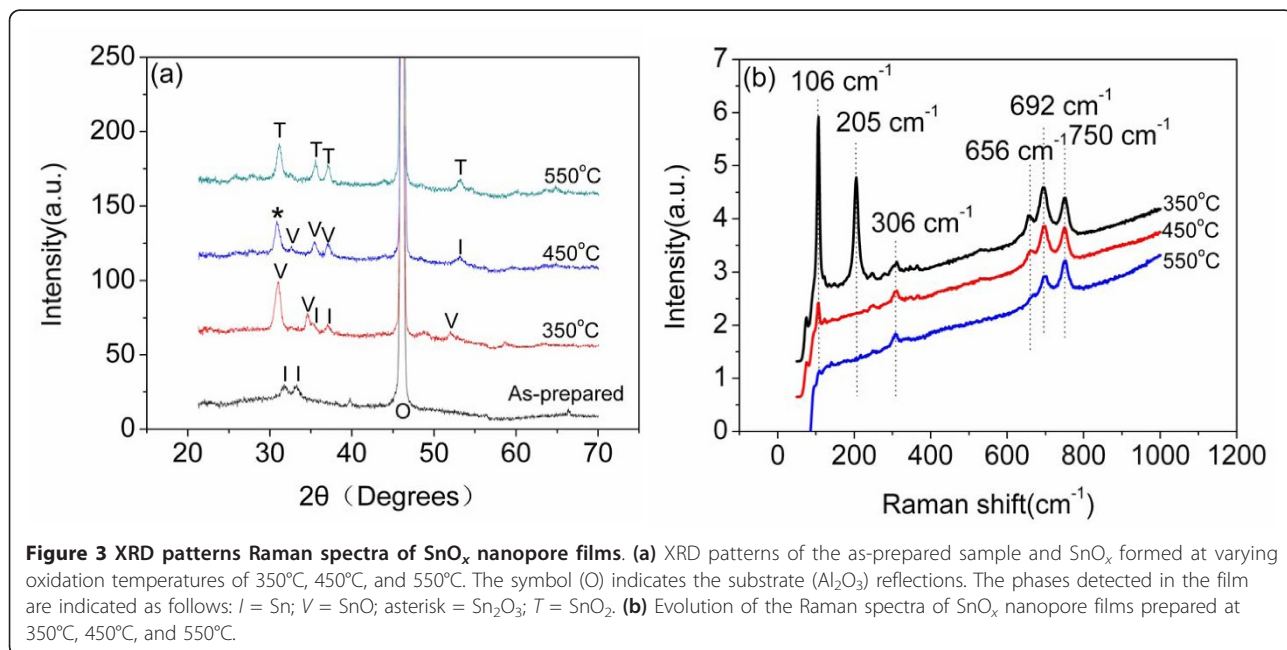
Composition evolution after annealing at different temperature

Figure 3a shows the XRD patterns of the Sn nanopore film deposited at room temperature and SnO_x films formed at different annealing temperatures (350°C, 450°C, and 550°C). It can be seen that the as-prepared Sn nanopore film consists only of metallic tin, and SnO is detected with a maximum contribution at 350°C. At the temperature of 450°C, the diffraction profile can be indexed by the reflections of SnO phase and Sn₂O₃ phase. This indicates that the SnO and Sn₂O₃ are simultaneously present at the annealing temperature of 450°C, and the intergrowth mechanisms may occur at this thermal oxidizing temperature. When the annealing temperature further increases to 550°C, the SnO and Sn₂O₃ diffraction peaks disappear, demonstrating that complete SnO₂ have been formed. This shows that the oxygen content of Tin oxide films prepared by annealing oxidizing is very relative to the annealing temperature. Figure 3b shows the Raman spectra in the Stocks

frequency range (50 to 1,000 cm⁻¹) for SnO_x films. The Raman spectrum of the sample annealed at 350°C contains strong peaks at approximately 750, 692, 656, 306, 205, and 106 cm⁻¹. The strongest peak at 106 and 206 cm⁻¹, which is typical of SnO, can be assigned to the B_{1g} (113 cm⁻¹) and A_{1g} (211 cm⁻¹) [17]. The bands peaking at 306, 692, and 750 cm⁻¹ can be correspond to SnO₂ modes E_u(TO), A_{2u}(LO), and E_u(LO) [18]. In addition to the fundamental Raman scattering peaks of rutile SnO₂, the other Raman scattering peaks, which are at about 656 cm⁻¹, are also observed. The origin of the 656 cm⁻¹ mode, which could not be clearly identified, might indicate other SnO_x stoichiometries. For sample annealed at 450°C, the SnO A_{1g} Raman modes disappears and B_{1g} Raman modes decreases, indicating the increase of oxygen in structures. Furthermore, the 656 cm⁻¹ mode and SnO B_{1g} mode disappear at the annealing temperature of 550°C, which shows the pure SnO₂ has formed. So the Raman spectra also demonstrate that the oxygen content increasing with the annealing temperature. The EDS analysis during FE-SEM observation reveals that the SnO_x films (prepared at 350°C, 450°C, and 550°C) have an approximate atomic ratio of tin to oxygen of 1:0.87, 1: 1.45, and 1:2, respectively. This is consistent with the results of XRD patterns and Raman spectra.

Photoresponse of the SnO_x nanopore films under UV irradiation

The room-temperature current-voltage (*I-V*) characteristics of the samples all showed a good ohmic behavior and the conductivity of the SnO_x films increase with rising annealing temperature (i.e., increasing film oxygen



content) at preparation. To investigate the photoresponse of the ordered SnO_x nanopore films under UV irradiation, the time-dependent measurements of photoresponse were employed to study the rise and decay time upon switching UV light on and off. After keeping the sample in the dark for 60 s under the constant voltage (1 V), we turn on the UV light to reach the maximum of the photocurrent and then turn off the light to

observe its recovery characteristics. The reproducibility of the sample was tested by repeatedly switching UV light on and off for the same time intervals. At the last cycle of the measurement, the photocurrent naturally returns to original value. Figure 4a, c shows the time evolution of current under UV lamp irradiation of a power of $I = 50 \mu\text{W cm}^{-2}$ at RT in air. The time-dependent photoresponse of sample prepared at 350°C reveals

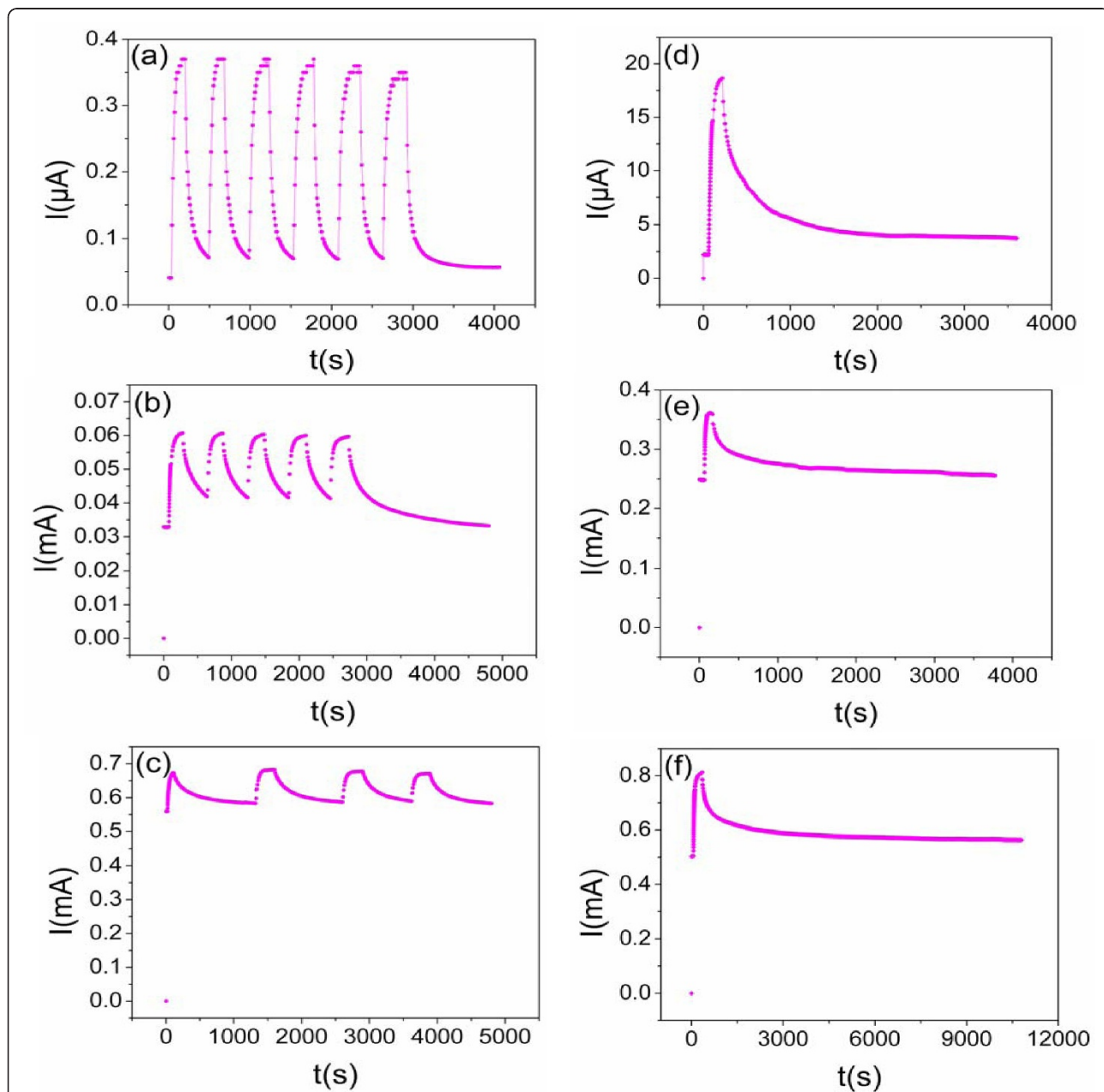


Figure 4 Time-dependent photoresponse of ordered SnO_x nanopore films and SnO_x thin films. (a, c) Time-dependent photoresponse of ordered SnO_x nanopore films annealed at 350°C, 450°C, and 550°C, respectively. (d, f) Time-dependent photoresponse of SnO_x thin films annealed at 350°C, 450°C, and 550°C, respectively. The measurements were carried out in dry air under 1-V bias voltage and approximately $50\text{-}\mu\text{W cm}^{-2}$ UV illumination.

a current increase steeply upon switching on UV light of more than ten times of magnitude (Figure 4a). The response time, defined as the time needed to reach 90% of the maximum photocurrent, was therefore about 52 s, and recovery time, defined as the time taken for the photocurrent to come within 10% of the initial value, about 270 s. Figure 4b shows the time-dependent photo-response of the sample prepared at 450°C. The response time and the recovery time were approximately 70 s and approximately 1,090 s, the current increase is about two times of magnitude in this case. For sample prepared at 550°C, a response time of approximately 62 s and a recovery time of approximately 3,350 s were obtained and the current increase is no more than one time of magnitude (Figure 4c). For SnO_x thin films, the response time and recovery time of the samples prepared at 350°C, 450°C, and 550°C are approximately 80 and 2,850 s, approximately 32 and 3,010 s, approximately 100 and > 10,450 s, respectively (Figure 4d, e, f). These results demonstrated that the ordered SnO_x nanopore film prepared at lower temperature possess higher UV light sensitivity and shorter current recovery time. What's more, the recovery time of ordered nanopore films is much shorter than that of thin films and reveal a good reversible switching characteristics with on/off UV exposure. Compared to SnO₂ nanowire-based UV detectors, the response and recovery performance of our UV detector (prepared at 350°C) was comparable to the SnO₂ nanowire array-based UV detector [19] and was still inferior to single nanowire UV detectors (the response time is less than 0.1 s) [20]. So there is still much work to do to further improve the performance of ordered SnO_x nanopore-film-based UV detectors in order to meet the practical application.

The decreased recovery time of the ordered SnO_x nanopore films compared to the thin films can be attributed to the increased surface areas. It is known that the oxygen molecules are absorbed onto SnO_x surface by capturing free electrons from the *n*-type SnO_x [$O_2(g) + e^- \rightarrow O_2^-(ad)$], which decrease the carrier density in the films and hence the porous films show a higher resistance. Upon UV illumination, electron-hole pairs are generated. The holes migrate to the surface along the potential slope produced by the band bending and recombine with the negatively charged adsorbed oxygen ions [$h^+ + O_2^- \rightarrow O_2(g)$], resulting in an enhancement of photocurrent. When the illumination is turned off, the films with higher surface area make O₂ read-sorbed on the surface easier, which lead to a shorter recovery time.

For the sample with a lower annealing, temperature shows a shorter recovery time, which could be attributed to below two main processes. First, it is known that oxygen vacancies in SnO_x act as electron donors and

the number of oxygen vacancies is expected to increase in lower annealing temperature under certain oxygen flows and annealing time (confirmed by the results of XRD pattern and Raman spectra above), higher concentration of the oxygen vacancies will give higher probability of the adsorption of oxygen molecules onto the surface of SnO_x films, leading to the fast decreasing of the photocurrent. Second, the increase in the oxygen vacancies is expected to decrease the bending of the semiconductor near the surface [21]. Electrons and holes recombine more easily with less bended band, inducing a shorter carrier lifetime. So the photocurrent decay after switching off UV is faster for the sample at lower annealing temperature.

Conclusions

In conclusion, we firstly report an effective method for the fabrication of ordered SnO_x nanopore films. Annealing temperature is the key factor to control Sn/O ratio. Reversible photoconductive switching characteristics of the films were exhibited by switching UV light on/off, which is ascribed to the oxygen desorption/reabsorption on the surface of SnO_x film. It is noted that the ordered SnO_x nanopore films with lower *x* value possess more excellent ability to detect weak UV light, which could be attributed to the higher concentration of the oxygen vacancies in this SnO_x films. Especially, this ordered nanopore films exhibit shorter recovery time compared to the thin films, which can be attributed to the increased surface areas. This study presents a new approach for fabricating UV light sensors based on Tin oxide films.

Abbreviations

AAO: anodized aluminum oxide; UV: ultraviolet; 2D: two-dimensional; DC: direct current; XRD: X-ray diffraction; FE-SEM: field-emission scanning electron microscope; EDS: energy disperse spectroscopy; RT: room temperature.

Acknowledgements

This work was supported by the National Major Basic Research Project of 2010CB933702, Natural Science Foundation of China (grant No. 11174197, 10874115, 10804071, and 10734020), National 863 Program 2011AA050518863, Shanghai Nanotechnology Research Project 0952nm01900, Research fund for the Doctoral Program of Higher Education of China. We thank Instrumental Analysis Center of SJTU for SEM analysis.

Author details

¹Laboratory of Condensed Matter Spectroscopy and Opto-Electronic Physics, Department of Physics, Shanghai Jiao Tong University, Shanghai, 200240, People's Republic of China ²School of Mechanical Engineering, Shanghai Dianji University, Shanghai 200240, People's Republic of China ³School of Chemistry and Chemical Technology, Shanghai Jiao Tong University Shanghai, 200240, People's Republic of China

Authors' contributions

CLL participated in the design of the study, carried out the total experiments, performed the statistical analysis, as well as drafted the manuscript. MJZ participated in the design of the study, provided the theoretical and experimental guidance, performed the statistic analysis, and

revised the manuscript. XHW helped to operate the Magnetron Sputtering System. LM participated in the design of experimental section and offered her the help in experiments. LJY provided helpful suggestion in the analysis of experimental data. WZS gave his help in the setting up of experimental apparatus. All authors read and approved the final manuscript.

Competing interests

The authors declare that they have no competing interests.

Received: 3 July 2011 Accepted: 6 December 2011

Published: 6 December 2011

References

1. Katsuki A, Fukui K: **H₂ selective gas sensor based on SnO₂.** *Sensor Actuator B: Chem* 1998, **52**:30-37.
2. Kolmakov A, Zhang Y, Cheng G, Moskovits M: **Detection of CO and O₂ using tin oxide nanowire sensors.** *Adv Mater* 2003, **15**:997-1000.
3. Law M, Kind H, Messer B, Kim F, Yang PD: **Photochemical sensing of NO₂ with SnO₂ nanoribbon nanosensors at room temperature.** *Angew Chem Int Ed* 2002, **41**:2405-2408.
4. Comini E, Faglia G, Sberveglieri G: **UV light activation of tin oxide thin films for NO₂ sensing at low temperatures.** *Sensor Actuator B: Chem* 2001, **78**:73-77.
5. Ferrere S, Zaban A, Gregg BA: **Dye sensitization of nanocrystalline tin oxide by perylene derivatives.** *J Phys Chem B* 1997, **101**:4490-4493.
6. Aoki A, Sasakura H: **Tin oxide thin film transistors.** *Jpn J Appl Phys* 1970, **9**:582.
7. Bond GC, Molloy LR, Fuller MJ: **Oxidation of carbon monoxide over palladium-tin(IV) oxide catalysts: an example of spillover catalysis.** *J Chem Soc Chem Comm* 1975, **19**:796-797.
8. Park MS, Wang GX, Kang YM, Wexler D, Dou SX, Liu HK: **Preparation and electrochemical properties of SnO₂ nanowires for application in lithium-ion batteries.** *Angew Chem* 2007, **119**:764-767.
9. Dai ZR, Gole JL, Stout JD, Wang ZL: **Tin oxide nanowires, nanoribbons, and nanotubes.** *J Phys Chem B* 2002, **106**:1274-1279.
10. Duan JH, Yang SG, Liu HW, Gong JF, Huang HB, Zhao XN, Zhang R, Du YW: **Single crystal SnO₂ zigzag nanobelts.** *J Am Chem Soc* 2005, **127**:6180-6181.
11. Hu JQ, Ma XL, Shang NG, Xie ZY, Wong NB, Lee CS, Lee ST: **Large-scale rapid oxidation synthesis of SnO₂ nanoribbons.** *J Phys Chem B* 2002, **106**:3823-3826.
12. Wang Y, Zeng HC, Lee JY: **Highly reversible lithium storage in porous SnO₂ nanotubes with coaxially grown carbon nanotube overlayers.** *Adv Mater* 2006, **18**:645-649.
13. Leite ER, Weber IT, Longo E, Varela JA: **A new method to control particle size and particle size distribution of SnO₂ nanoparticles for gas sensor applications.** *Adv Mater* 2000, **12**:965-968.
14. Ying Z, Wan Q, Song ZT, Feng SL: **SnO₂ nanowhiskers and their ethanol sensing characteristics.** *Nanotechnology* 2004, **15**:1682-1684.
15. Sun FQ, Cai WP, Li Y, Jia LC, Lu F: **Direct growth of mono- and multilayer nanostructured porous films on curved surfaces and their application as gas sensors.** *Adv Mater* 2005, **17**:2872-2877.
16. Li YB, Zheng MJ, Ma L, Shen WZ: **Fabrication of highly ordered nanoporous alumina films by stable high-field anodization.** *Nanotechnology* 2006, **17**:5101-5105.
17. Geurts J, Rau S, Richter W, Schmitte FJ: **SnO films and their oxidation to SnO₂: Raman scattering, IR reflectivity and X-ray diffraction studies.** *Thin Solid Films* 1984, **121**:217-225.
18. Diéguez A, Romano-Rodríguez A, Vilà A, Morante JR: **The complete Raman spectrum of nanometric SnO₂ particles.** *J Appl Phys* 2001, **90**:1550-1557.
19. Wu JM, Kuo CH: **Ultraviolet photodetectors made from SnO₂ nanowires.** *Thin Solid Films* 2009, **517**:3870-3873.
20. Liu ZQ, Zhang DH, Han S, Li C, Tang T, Jin W, Liu XL, Lei B, Zhou CW: **Laser ablation synthesis and electron transport studies of tin oxide nanowires.** *Adv Mater* 2003, **15**:1754-1757.
21. Vlachos DS, Papadopoulos CA, Avaritsiotis JN: **Dependence of sensitivity of SnO_x thin-film gas sensors on vacancy defects.** *J Appl Phys* 1996, **80**:6050-6054.

doi:10.1186/1556-276X-6-615

Cite this article as: Li et al.: Fabrication and ultraviolet photoresponse characteristics of ordered SnO_x (x ≈ 0.87, 1.45, 2) nanopore films. *Nanoscale Research Letters* 2011 **6**:615.

Submit your manuscript to a SpringerOpen® journal and benefit from:

- Convenient online submission
- Rigorous peer review
- Immediate publication on acceptance
- Open access: articles freely available online
- High visibility within the field
- Retaining the copyright to your article

Submit your next manuscript at ► springeropen.com